GEOPHYSICAL RESEARCH LETTERS, VOL. 22, NO. 12, PAGES 1569-1572, JUNE 15, 1995

Thermal infrared lightcurves of the impact of Comet Shoemaker-Levy 9 fragment R

A. J. Friedson,[1] W. F. Hoffmann,[2] J. D. Goguen,[1] L. K. Deutsch,[3] G. S. Orton,[1] J. L. Hora,[4] A. Dayal,[2] J. N. Spitale,[5] W. K. Wells,[6] and G. G. Fazio[7]

Abstract. The impact of fragment R was observed at thermal infrared wavelengths of 7.85, 10.3 and 12.2 μm from the NASA/Infrared Telescope Facility on July 21 UT, using the MIRAC2 mid-infrared array camera. Thermal emission at the three wavelengths was sampled sequentially using a 1.8% circular variable filter, with an average time interval of 17 seconds between observations at different wavelengths. Continuous imaging of Jupiter in this mode began at 5:08 UT and extended to 5:55 UT. We present calibrated lightcurves for the three wavelengths. Clear evidence for enhanced emission from the impact region first appears at 5:41 UT, with the peak in emission at all three wavelengths occurring ~3.5 minutes later. The information content of the data is presented in terms of plots of the product of emissivity times angular size *versus* source temperature for each wavelength. Assuming that the peak in the lightcurves is due to rotation of the hot impact site into view from Earth, we estimate a diameter of ~1900 km for the source emitting area at 5:44:30 UT and estimate a lower limit on the source temperature at this time of ~1350 K. This lower limit drops to 800 K if the diameter of the emitting region was actually a factor of two larger.

Introduction

One of the principal goals of the Comet Shoemaker-Levy 9 observing program at the NASA Infrared Telescope Facility (IRTF) was to search for and characterize excess near- and mid-infrared emission generated during and just after the impacts of comet fragments B, C, F, G, R, V, and W with Jupiter's atmosphere. A preliminary analysis of these data is contained in a synopsis of the entire IRTF SL9 campaign [*Orton et al.*, 1995]. Here we present a more thorough analysis of our mid-infrared observations of the impact of fragment R.

[1] Jet Propulsion Laboratory, Pasadena, CA
[2] Steward Observatory, University of Arizona, Tucson, AZ
[3] FCAD, University of Massachusetts, Amherst, MA
[4] Institute for Astronomy, University of Hawaii, Honolulu, HI
[5] California Institute of Technology, Pasadena, CA
[6] Lunar and Planetary Laboratory, University of Arizona
[7] Smithsonian Astrophysical Observatory, Boston, MA

Paper number 95GL00359
0094-8534/95/95GL-00359$03.00

At wavelengths longward of 5 μm, we were assured of detecting only thermal emission; in comparison, sunlight scattered off particulates at these wavelengths would be negligible, even if the cloud of particles was optically thick. This was the primary reason for our choice to observe the impact at mid-IR wavelengths. Another motivation was the desire to merge this experiment smoothly with a search for impact-generated seismic waves made in the 7-μm region.

Observations

The impact of fragment R was observed on July 21 UT using the MIRAC2 mid-infrared array camera at the IRTF 3.0-meter Cassegrain focus. MIRAC2 is a Si:As impurity-band conduction array with a 128×128 pixel format. Its predecessor, MIRAC1, is described by *Hoffmann et al.* [1993]. The plate scale at the IRTF was approximately 0.38 arcsec/pixel. Subtraction of sky emission was accomplished by nodding the telescope on and off the source. Jupiter's radiances at 7.85, 10.3, and 12.2 μm were sampled sequentially using a 1.8% circular variable filter, with an average time interval of 17 seconds between observations at different wavelengths. The total integration time was 1.96 sec at each wavelength. Continuous imaging in this mode began at 5:08 UT and extended to 5:55 UT, after which measurements were made more often at 7.85 μm than at the other wavelengths for the purposes of a seismic wave search. Absolute times were read off the local computer network whenever the MIRAC2 computer was rebooted. The network time was calibrated to within 2 seconds early during the impact week.

Data Reduction

The first step in processing the raw images involved correcting for pixel-to-pixel variations in the sensitivity of the array. This correction was carried out by taking the difference of two images of even illumination but significantly different intensity. The resulting image was normalized to an average value of 1.0 to produce the final "gain matrix". Each image was then divided by the gain matrix to yield a new image of approximately the same average value but with the signal in each pixel adjusted up or down based on that pixel's sensitivity relative to the average sensitivity of the entire array.

The images were next corrected for variations of that part of the sky emission not completely cancelled by the nod subtraction. The raw data were averaged over 4.2×4.2 arcsec square apertures centered on Jupiter's disk and on two patches of sky located in the southeast

Table 1. Comparison of Calibrations of Jupiter's Disk-Average Intensity for 1994 August 5 and August 6 UT

λ (μm)	Flux Density, α Boo (10^{-15} W cm^{-2} μm^{-1})	I, August 5 (10^{-6} W cm^{-2} μm^{-1} sr^{-1})	I, August 6 (10^{-6} W cm^{-2} μm^{-1} sr^{-1})	Difference %
7.85	5.00	1.73	1.66	4.1
10.50	1.75	2.34	2.26	3.5
10.73	1.60	2.31	2.47	6.3
12.20	0.98	6.21	6.03	2.9

and northwest corners of the images. Time variations of the signals in each aperture displayed a high degree of correlation. In addition, the background levels in the two widely separated patches of sky were nearly equal most of the time at each wavelength, indicating that the residual sky emission did not vary substantially over the field of view and that its subtraction from the raw center-of-disk (COD) signal is justified. The background-corrected COD flux does not vary as rapidly with time as the background, but does vary significantly on a time scale of ~10 minutes. We attribute this variation to changes in the transmission of the terrestrial atmosphere, since real changes of this magnitude in Jupiter's average COD brightness over such short time scales are precluded by Jupiter's high degree of longitudinal axisymmetry and sluggish thermal response time [*Orton et al.*, 1991; *Orton et al.*, 1994]. Since Jupiter's true COD brightness was nearly constant over the observing period, we used the observed variation of the background-corrected COD signal as a "running" calibrator for the observations. This required an accurate determination of the Jovian average COD brightness for July 21.

The sky over Mauna Kea on the day of the impact was not photometric in the mid-IR, so we were forced to rely on observations of Jupiter acquired under good conditions on August 5 and 6 UT to determine the disk-averaged radiance. We have assumed that the measured disk-averaged radiance was not significantly dependent on the sub-earth longitude at the observation time and that it did not change significantly over the ~2 week interval between late July and early August. The assumption about the axisymmetry of the disk-averaged radiance was tested to some extent by comparing the August 5 calibration to that of August 6, where the data were taken on opposite faces of the planet. Table 1 displays the disk-averaged radiance $\overline{I}$ determined for August 5 and 6. Also shown is the flux we used for our standard star, α Boo. A correction was made for any old impact sites appearing on the disk, but it never amounted to more than 1% of the computed disk average. The values of $\overline{I}$ obtained for the two days agree to better than 6.5% despite having been measured on separate days and on opposite hemispheres of the planet. The degree to which $\overline{I}$ could have changed over the two week time interval is uncertain. A decade of thermal infrared observations of Jupiter's troposphere and stratosphere [*Orton et al.*, 1991; *Orton et al.*, 1994] have not revealed any phenomena that would significantly change $\overline{I}$ on this short of a time scale; at this time, our assumption concerning the temporal steadiness of $\overline{I}$ is based solely on this experience.

A glance at Table 1 indicates that data on August 5 and 6 UT were taken at 10.5 and 10.73 μm rather than at 10.3 μm. Using the August data to calibrate the July 21 10.3-μm data thus required a relationship to be established between Jupiter's radiance at this wavelength and at 10.5 and 10.73 μm. Voyager IRIS spectra [*Hanel et al.*, 1979] were used for this purpose. When the spectral resolution of the IRIS data is degraded to match the 1.8% CVF resolution, the 10.3 to 10.5 μm brightness ratio (when the radiance is in the units used in Table 1) is found to be 0.94 in a belt and 0.90 in a zone, while the 10.3 to 10.73 μm ratio is 0.98 in a belt and 0.92 in a zone. For the disk average ratio, we have taken the average of the belt and zone ratios. We used these ratios to determine the 10.3 μm radiance on August 5 and 6. The result found for August 6 differed from August 5 by 5.8%. Averaging the results for the two days gave $\overline{I}$ equal to 1.69×10^{-6}, 2.18×10^{-6}, and 6.12×10^{-6} W cm^{-2} μm^{-1} sr^{-1} for 7.85, 10.3, and 12.2 μm, respectively. The background-corrected, disk-averaged signal on Jupiter for July 21 was computed for pre-impact

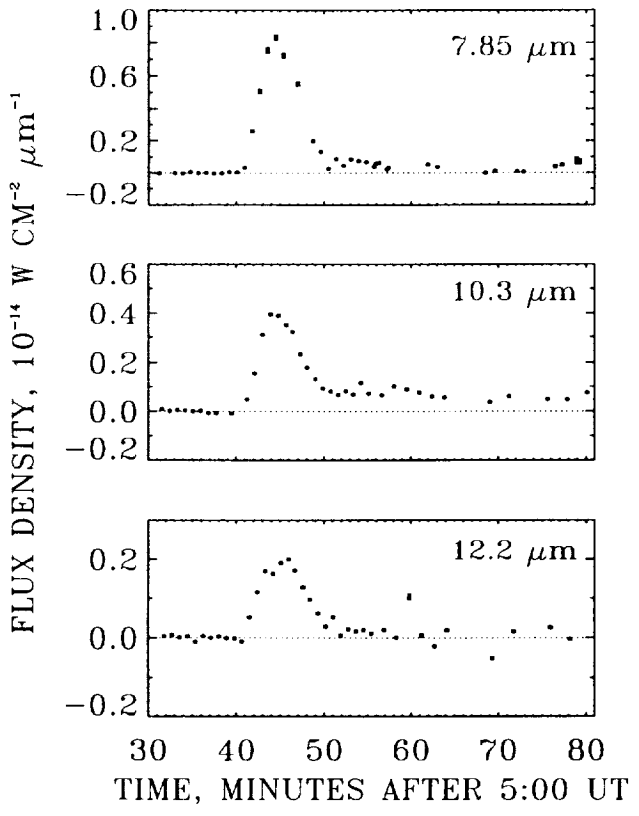

Figure 1. Flux Density versus time for the three wavelengths. The error bars, at times smaller than the plot symbols, represent one standard deviation of random error, which is dominated by the standard deviation of the background signal over the array. The systematic error associated with the uncertainty in the calibration, of order ~12%, generally dominates the random errors.

images acquired between 4:58 and 5:33 UT, after correcting for the old impact sites that were visible on the disk. The ratio of the average COD signal to the disk-averaged signal was computed for each image, and the average COD brightness was computed as the product of this ratio and the disk-averaged brightness obtained from August. The median and average absolute deviation of the COD brightness at each wavelength calculated over the set of pre-impact images was found to be 1.54±0.06, 2.29±0.01, and 6.23±0.06 in units of 10^{-6} W cm^{-2} μm^{-1} sr^{-1} for 7.85, 10.3, and 12.2 μm, respectively. The calibration constant for each image was then determined as the ratio of this brightness to the background-corrected COD signal. Our estimate for the accuracy of this calibration is ~12% for each wavelength.

Lightcurves

The lightcurve at each wavelength was computed by first summing measured pixel intensities over a 4.2×4.2 arcsec aperture centered on the impact position. The time average of summed intensities in the same aperture occurring before 5:40 UT was then subtracted from the data at all times to isolate the excess emission created by the impact. The lightcurve for each wavelength is shown in Figure 1 for times between 5:30 and 6:20 UT. After 5:53 UT, the sky emission became highly time variable and also somewhat spatially variable over the field of view of the camera, making background subtraction at these times difficult, particularly at 12.2 μm. Hence, interpretation of the data at these times must be done with caution.

The average sampling time between measurements at the same wavelength was 51 seconds. At this time resolution, the lightcurves have a similar shape and timing as those seen at near-IR wavelengths [*Graham et al.*, 1995]. The first clear evidence for the onset of the bright flare (we will use the term "flare" to denote the major brightening event seen in lightcurves throughout the infrared) appears in a 7.85 μm image taken at 5:40:57 UT. A 12.2 μm image taken 17 seconds earlier shows no signs of enhanced emission, while strong excess emission appears at all three wavelengths after 5:41 UT. The bright flare onset time at 2.3 μm is reported by *Graham et al.* to occur at 5:40:57 UT as well.

The peak of the flare at 7.85 μm occurs at 5:44:30 UT, within our 51-second time resolution of the 2.3 μm peak occurring at 5:44:57 [*Graham et al.*, 1995]. The peak emission at 10.3 μm occurs sometime between 5:43:50 and 5:44:50 UT and hence appears to precede the peak at 2.3 μm by 7 to 67 seconds. The 12.2 μm lightcurve displays two local maxima, one occurring at 5:43:20 and the other at 5:46 UT. By 5:50 UT, the excess emission from each wavelength has decreased to less than 16% of the peak value. There is evidence that the excess emission from the impact was sustained for at least another 5-6 minutes; however, there may be a significant contribution during this time interval from old impact sites associated with the D and G fragments, which are not spatially resolved from the R impact site during this time period.

There is an increase of the 7.85 μm signal at the planetary limb at the impact latitude at 5:36:33 and in the subsequent sample at 5:37:25 whose amplitude is 0.2% of the peak signal for the event. There are also increases of the signal at 10.3 and 12.2 μm in the two samples preceding the first 7.85 μm sample, but these are less distinguishable from the noise level. To within our time resolution, these increases are coincident with the second flash observed at the Keck telescope [*Graham et al.*, 1995] between about 5:36 and 5:38 UT.

Discussion

The data set presented here is not sufficient by itself for a unique determination of the physical size and temperature of the emission region. The major obstacles to determining these characteristics include our present lack of knowledge concerning the source geometry and the nature and distribution of the gaseous and particulate opacity, both of which vary with time. A simple model for the lightcurves is given by the system of equations

$$F_\lambda(\lambda_i) = \epsilon_\lambda(\lambda_i)\Omega B_\lambda(T, \lambda_i) \quad (1)$$

where λ_i = 7.85, 10.3, or 12.2 μm, F_λ is the measured flux density, ϵ_λ is the emissivity averaged over the CVF bandpass, Ω is the apparent angular size of the source, T is the effective source temperature, and B_λ is the Planck function. All the variables are functions of time. In the above system, we have assumed that the source is in local thermodynamic equilibrium (LTE), and that the emission at all three wavelengths can be adequately represented at any time by a single angular size and emitting temperature. The validity of these assumptions can only be assessed when the full complement of

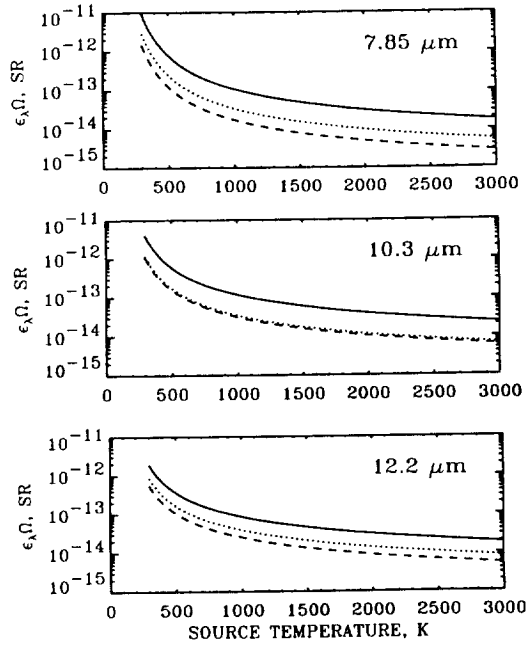

Figure 2. The product of emissivity times angular size $\epsilon_\lambda\Omega$ is plotted against assumed source temperature for three times during the impact event. Dotted curve, 5:42 UT. Solid curve, 5:44:30 UT. Dashed curve, 5:50 UT. Since the emissivity can never exceed unity, these curves are useful for setting a lower limit in the angular size, given the source temperature, or on the source temperature, given the angular size.

observations of the R impact have been analyzed as a whole.

If we accept Equation (1) as an adequate model, then the information content of the data can be displayed in a plot of the product $\epsilon_\lambda \Omega$ vs. T. Figure 2 shows such curves for each wavelength, for three different times during the bright flare. These curves relate any one of the three unknowns ϵ_λ, Ω, or T to the other two for a particular wavelength. Perhaps of more importance is the fact that, since the emissivity can never exceed unity, the curves can be used to establish a lower limit for the angular size, given the source temperature, or a lower limit for the source temperature, given the angular size.

Additional information concerning the source angular size may be derived from examining the timing of features in the lightcurves and from near-IR data. The onset of the bright flare must be due to a strong increase in the intrinsic brightness of the source, an increase in its angular size, or both. Here we adopt the view of *Graham et al.* that the flare is due primarily to an increase in the angular size associated with rotation of the hot impact site into view from Earth, and consider the implications for the physical size of the emitting area. According to this model, the onset of the flare occurs when the leading edge of the impact site begins to rise over Jupiter's eastern limb and the peak of the flare represents roughly the time when the trailing edge rotates past the limb. The elapsed time between the onset and peak of the flare at 7.85 μm is ~210 sec. Assuming that the size of the emission region did not vary appreciably during this time interval, we find a diameter for the impact site of ~1800 km. This diameter can also be obtained in another way. *Graham et al.* report the appearance of a bright flash at 5:34:45 UT which they associate with the initial meteor streak of fragment R. If this interpretation is correct, then the elapsed time between the impact time and the onset of the flare would be 370 sec. According to the calculations of *Chodas and Yeomans* (unpublished data, July 20, 1994), fragment R struck Jupiter 4.9° behind the limb. After 370 sec, the center of the impact site would still be 1.2° behind the limb. For the onset of the flare to be seen 370 sec after the impact, the diameter of the emitting area would have to be ~2000 km. The two estimates for the spatial scale of the emitting region are seen to agree fairly well, given the simplicity of the model. By a similar argument, *Graham et al.* estimated a diameter of about 1300 km. The difference between their derived diameter and ours stems from their use of 150 sec as the time scale for the flare brightness increase, whereas we have used 210 sec based on the 7.85 μm lightcurve.

A circular disk of diameter 1900 km, the trailing edge of which has just cleared the limb, at the latitude of the impacts would have an angular size of 6×10^{-14} sr. The time at which this happens corresponds to the peak of the flare. Referring to Fig. 2, the 7.85-μm data require that a feature with an angular size of 6×10^{-14} sr at 5:44:30 UT would have to have had a source temperature of at least 1350 K. If the source brightness was decreasing while the feature rotated into view, then our estimate of the diameter of the emitting area given above would be too low. If the true diameter of the emitting area were a factor of two larger, the lower limit on the source temperature at 5:44:30 UT would drop to 800 K.

Graham et al. report that the R impact site was spatially resolved by the Keck telescope by 5:50 UT and estimate a linear dimension for the impact site at this time of ~7500 km. This estimate can probably not be viewed as accurate to better than 50%, on account of the seeing. If we take 11000 km as the largest the impact site could have been at 5:50 UT, assume a flat circular disk geometry, and note that the center of the feature at this time would have been 4° beyond the limb on the Earth-facing hemisphere, we derive an angular size of 7.7×10^{-12} sr. From Fig. 2, the lower limit for the source temperature is found to be ~300 K.

Many of the estimates derived in this section had to be based on assumptions concerning the shape and emitting area of the source. Fortunately, emission from the impact of fragment R was observed from many ground-based observatories, from the Kuiper Airborne Observatory, and by the NIMS, PPR, and UVS instruments aboard the Galileo spacecraft. Hence, there is every reason to be optimistic that our knowledge of the R impact will improve as these various data sets are analyzed and the results are published.

Acknowledgments. The authors wish to thank Robert Joseph for his enthusiastic support of comet impact science at the IRTF. We acknowledge support from the NASA Planetary Astronomy Program and National Science Foundation. The MIRAC2 upgrade to the 128×128 array was also supported by Steward Observatory, U. Arizona, and by the Smithsonian Astrophysical Observatory. All of the authors were visiting astronomers at the Infrared Telescope Facility, which is operated by the University of Hawaii under contract to the National Aeronautics and Space Administration.

References

Graham, J.R., I. de Pater, J.G. Jernigan, M.C. Liu, and M.E. Brown, W.M. Keck Telescope observations of the Comet P/Shoemaker-Levy 9 Fragment R Jupiter Collision, *Science, in press*, 1995.

Hanel, R., and 12 others, Infrared observations of the Jovian system from Voyager 1, *Science, 204*, 972-976, 1979.

Hoffmann, W.F., G.G. Fazio, K. Shivanandan, J.L. Hora, and L.K. Deutsch, Astronomical observations with the Mid-InfraRed Array Camera MIRAC, *Infrared Phys. Technol., 35*, 175-194, 1993.

Orton, G.S., and 14 others, Thermal maps of Jupiter: Spatial organization and time dependence of stratospheric temperatures, 1980 to 1990, *Science, 252*, 537-542, 1991.

Orton, G.S., and 18 others, Spatial organization and time dependence of Jupiter's temperatures, 1980-1993, *Science, 265*, 625-631, 1994.

Orton, G.S., and 54 others, The NASA Infrared Telescope Facility investigation of Comet Shoemaker-Levy 9 and its Collision with Jupiter: Preliminary results, *Science, in press*, 1995.

A. J. Friedson, MS 169-237, Jet Propulsion Laboratory, Pasadena, CA 91109; ajf@maui.jpl.nasa.gov

(received December 5, 1994; revised December 30, 1994; accepted January 5, 1995.)